ORIGINAL CONTRIBUTION

The effect of step-stretch parameters on capillary breakup extensional rheology (CaBER) measurements

Erik Miller · Christian Clasen · Jonathan P. Rothstein

Abstract Extensional rheometry has only recently been developed into a commercially available tool with the introduction of the capillary breakup extensional rheometer (CaBER). CaBER is currently being used to measure the transient extensional viscosity evolution of mid to low-viscosity viscoelastic fluids. The elegance of capillary breakup extensional experiments lies in the simplicity of the procedure. An initial step-stretch is applied to generate a fluid filament. What follows is a self-driven uniaxial extensional flow in which surface tension is balanced by the extensional stresses resulting from the capillary thinning of the liquid bridge. In this paper, we describe the results from a series of experiments in which the step-stretch parameters of final length, and the extension rate of the stretch were varied and their effects on the measured extensional viscosity and extensional relaxation time were recorded. To focus on the parameter effects, well-characterized surfactant wormlike micelle solutions, polymer solutions, and immiscible polymer blends were used to include a range of characteristic relaxation times and morphologies. Our experimental results demonstrate a strong dependence of extensional rheology on step-stretch conditions for both wormlike micelle solutions and immiscible polymer blends. Both the extensional viscosity and extensional relaxation time of the wormlike micelle solutions were found to decrease with increasing extension rate and strain of the step-stretch. For the case of the immiscible polymer blends, fast step-stretches were found to result in droplet deformation and an overshoot in the extensional viscosity which increased with increasing strain rates. Conversely, the polymer solutions tested were found to be insensitive to step-stretch parameters. In addition, numerical simulations were performed using the appropriate constitutive models to assist in both the interpretation of the CaBER results and the optimization of the experimental protocol. From our results, it is clear that any rheological results obtained using the CaBER technique must be properly considered in the context of the stretch parameters and the effects that preconditioning has on viscoelastic fluids.

Keywords Capillary rheometer · Wormlike micelles · Polymer blend · Elongational flow

Introduction

The elegance of capillary breakup extensional rheometry (CaBER) experiments lies in the simplicity of the procedure. A step-stretch is applied, after which the experiment drives itself as capillary thinning of the liquid bridge imposes a uniaxial extensional flow on the fluid filament. The decay of the filament diameter, from which all properties are calculated, is measured until capillary pinch-off brings the experiment to an end. However, it should come as no surprise that a number of viscoelastic fluids are greatly affected by the parameters of the initial step-stretch. In this paper, we will investigate the role of step-stretch parameters

E. Miller · J. P. Rothstein (✉)
Department of Mechanical and Industrial Engineering,
University of Massachusetts, Amherst, MA 01003, USA
e-mail: rothstein@ecs.umass.edu

C. Clasen
Department of Chemical Engineering, Katholieke
Universiteit Leuven, 3001 Leuven, Belgium

and the resulting extensional preconditioning on three classes of fluids: polymer solutions, wormlike micelle solutions, and immiscible polymer blends.

Although little is known about the effect of extensional preconditioning on extensional rheology, there have been some recent extensional experiments with shear flow preconditioning performed on both polymer solutions and viscoelastic wormlike micelle solutions although no such experiments exist for immiscible polymer blends. The transient evolution of macromolecular microstructure is very sensitive to the initial configuration of the macromolecule, a concept known as "molecular individualism" (Doyle et al. 1998; Smith and Chu 1998). Numerical simulations have also shown that the imposition of either an oscillating extensional field or a pre-shear in the direction of stretch on a polymer solution reduces the occurrences of kinks and folds, resulting in faster stretching during subsequent extensional flows (Larson 2000). Several studies have attempted to experimentally quantify the effect of pre-shear history on the response of complex fluids in extensional flows (Anna 2000; Anna and McKinley 2008; Bhardwaj et al. 2007b; James et al. 1987; Vissmann and Bewersdorff 1990).

Anna (Anna 2000; Anna and McKinley 2008) used a pre-shear device attached to the upper plate of a filament stretching rheometer (FiSER) to quantitatively determine the effect of pre-shearing on the extensional behavior of a series of polystyrene Boger fluids. Anna's experiments demonstrated that the pre-shear results in a delay of the onset of strain hardening of the extensional viscosity; a result that is confirmed by FENE-P and the Brownian dynamic simulations of Larson (2000, 2005) and Agarwal (2000). The delay in strain hardening can be explained as stemming from the need for the deformed polymers to either rotate from the shear direction into the stretch direction or, alternately, to compress back through its equilibrium conformation before it is subsequently stretched.

In Bhardwaj et al. (2007b), the role of pre-shear on the extensional rheology of a series of wormlike micelle solutions was studied using both FiSER and CaBER. As was observed with polymer solutions, increasing the strength and the duration of the pre-shear prior to FiSER was found to result in a delay in the onset of strain hardening to larger Hencky strains. However, the wormlike micelle solutions were observed to be significantly more sensitive than polymer solutions to pre-shear. Bhardwaj et al. (2007b) hypothesized that the increased sensitivity of the wormlike micelle solutions was a direct result of pre-shearing either reducing the size of the wormlike micelles or changing the interconnectivity of the micelle network prior to stretch.

Interestingly, the effect of pre-shear on the extensional viscosity of wormlike micelle solutions measured in the capillary breakup rheometry experiments was observed to be very different from that observed in filament stretching. The solutions were found to strain-harden faster, achieve larger steady-state extensional viscosities and an increase in the extensional relaxation time with increasing pre-shear rate and duration. The difference between the response of the wormlike micelles in FiSER and CaBER experiments demonstrates the sensitivity of these self-assembling systems not only to pre-shear but also to the exact dynamics of the stretch profile. The extensional flow imposed in a controlled FiSER stretch is homogeneous as the instrument is capable of controlling and setting constant stretch rates. CaBER experiments on the other hand are inhomogeneous after the step-stretch and self-select their stretch rate profile that reflects the natural thinning dynamics of a liquid filament. The experiments by Bhardwaj et al. (2007b) highlight the difficulty in properly designing a CaBER experiment and interpreting the resulting data for complex liquids such as self-assembling wormlike micelle solutions. Additionally, these pre-shear experiments were the main motivation for the in-depth study into the role of step-stretch conditions on the extensional rheology measurements of different classes of complex fluids presented in this paper. As CaBER measurements are a relatively new technique, the goal of this study was to isolate a definitive range of step-stretch parameters for which the extensional rheology measurements are relatively insensitive and repeatable.

Experimental setup

Capillary breakup extensional rheology

Capillary breakup extensional rheometry measurements have become an increasingly common technique for determining the extensional rheology of the less concentrated and less viscous fluids (Anna and McKinley 2001; Bazilevsky et al. 1990; Clasen et al. 2006; Entov and Hinch 1997; Kojic et al. 2006; McKinley and Tripathi 2000; Plog et al. 2005; Rodd et al. 2005; Stelter et al. 2000; Yesilata et al. 2006). The capillary breakup extensional rheometry measurements presented here were performed using both a filament stretching rheometer (Rothstein 2003; Rothstein and McKinley 2002) as well as the commercially available HAAKE CaBER 1 produced by Thermo Fisher Scientific. In all of the CaBER experiments presented here, an initial nearly cylindrical fluid sample is placed

between two cylindrical plates and stretched with an exponential profile, $L = L_0 \exp(\dot{\varepsilon}_0 t)$, at a constant extension rate $\dot{\varepsilon}_0$ from an initial length L_0 to final length of L_f. The stretch is then stopped and the capillary thinning of the liquid bridge formed between the two endplates produces a uniaxial extensional flow that can be used to measure an apparent extensional viscosity of the test fluid. A schematic diagram of the stretch is shown in Fig. 1. In order to test the sensitivity of the extensional viscosity measurements to the final length of the step-stretch, a range of stretch ratios between $3 \leq L_f / R_0 \leq 15$ were chosen. Additionally, a range of extension rates were imposed such that for the elastic test fluids like wormlike micelle solutions and polymer solutions which have a relaxation time, λ, the Weissenberg number was between $0.5 < Wi = \lambda \dot{\varepsilon} < 12$ and for the immiscible polymer blends the imposed extension rates were between $1\,\mathrm{s}^{-1} < \dot{\varepsilon} < 40\,\mathrm{s}^{-1}$. All the resulting stretch rates were greater than the inverse timescale for capillary drainage of the liquid bridge, $\dot{\varepsilon} > \sigma / \eta_0 R_0$, as necessary in order to observe the thinning process (Anna and McKinley 2001).

The breakup of the fluid filament is driven by capillary stresses and resisted by the extensional stresses developed within the flow. The extensional viscosity of a complex liquid solution can be determined by measuring the change in the filament diameter as a function of time. Papageorgiou (1995) showed that for a Newtonian fluid of extensional viscosity η_E the radius of the fluid filament will decay linearly with time, $R_{\mathrm{mid}}(t) \propto (t_b - t)/\eta_E$, to the final breakup at t_b. Conversely, Entov and Hinch (1997) showed that for an Oldroyd-B fluid with an extensional relaxation time λ_E, the radius will decay exponentially with time, $R_{\mathrm{mid}}(t) \propto \exp(-t/3\lambda_E)$, resulting in a constant extension rate of the fluid filament given by

$$\dot{\varepsilon} = -\frac{2}{R_{\mathrm{mid}}(t)} \frac{dR_{\mathrm{mid}(t)}}{dt} = \frac{2}{3\lambda_E}; \tag{1}$$

$L = L_0 \exp(\dot{\varepsilon}_0 t)$

R_{mid}

L_o

$t = 0$

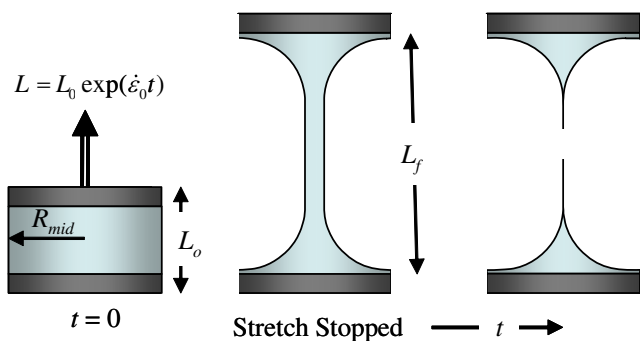Stretch Stopped — t ⟶

L_f

Fig. 1 Schematic diagram of capillary breakup extensional rheology (CaBER) experiment

hence, for an Oldroyd-B fluid, the flow has a constant Weissenberg number of $Wi = \lambda_E \dot{\varepsilon} = 2/3$. This value is larger than the critical Weissenberg number of $Wi = 1/2$ needed to achieve coil-stretch transition and thus the uniaxial extension should be fast enough to produce strain hardening of the extensional viscosity at this constant extension rate of both the wormlike micelle solution and the polymer solutions. In general, however, we observe, over the course of the experiment, a transition between these two limiting cases and the observed extension rate is not constant, but a function of time. The thinning dynamics that the fluid chooses depend on the deformation history of the viscoelastic system and the resulting stress evolution in the filament. Still, the evolution of an *apparent* extensional viscosity with this extension rate profile can easily be calculated by applying a force balance between capillary stresses and the viscous and elastic tensile stresses within the fluid filament (Anna and McKinley 2001)

$$\eta_E = \frac{\sigma / R_{\mathrm{mid}}(t)}{\dot{\varepsilon}(t)} = \frac{-\sigma}{dD_{\mathrm{mid}}/dt}. \tag{2}$$

To calculate the apparent extensional viscosity, the diameter measurements can either be fit with a spline and then differentiated numerically as is the case with the HAAKE CaBER 1 results presented for the immiscible polymer blends or, for more well-defined fluids, the diameter can first be fit with an appropriate functional form and then be differentiated with respect to time. Of course, choosing a specific function can mask some of the details in the diameter decay data and should only be employed when an excellent quantitative fit to the data can be obtained. For the case of viscoelastic systems where the elastic component reaches a finite extensibility, for example, the polymer chains in a Boger fluid, Anna and McKinley (2001) proposed the following fitting function:

$$D_{\mathrm{mid}}(t) = Ae^{-Bt} - Ct + E. \tag{3}$$

The choices of fitting parameters in Eq. 3 have some physical relevance. The exponential decay of the fluid filament diameter at intermediate times can be related to the extensional relaxation time and the fitting parameter B such that $B = 1/3\lambda_E$. For Boger fluids and dilute polymer solution systems, this extensional relaxation time can be much larger than the shear relaxation time (Clasen et al. 2006). Additionally, C can be related to the equilibrium value of the extensional viscosity at late times, $\eta_{E,\infty}$, when the finite extensibility limit of the polymer is reached, such that $C = 0.7127\sigma/\eta_{E,\infty}$ (Papageorgiou 1995).

Test fluids

The role of step-stretch parameters and the resulting extensional preconditioning in CaBER was investigated on three different classes of fluids: polymer solutions, wormlike micelle solutions, and immiscible polymer blends.

The polymer solution used was a 1-wt.% high molecular weigh polyacrylamide (PAA; $M_w = 6 \times 10^6$ g/mol; Scientific Polymer Products) in Millipore-filtered water. The full shear rheology is reported elsewhere (Edmond et al. 2006); however, for completeness, the zero shear viscosity, relaxation time, storage modulus, and surface tension for each of the fluids are listed in Table 1.

The wormlike micelle solutions tested were composed of the cationic surfactant cetylpyridinium chloride (CPyCl; Fisher Scientific) and sodium salicylate (NaSal; Fisher Scientific) dissolved in a solution of 100 mM NaCl in distilled water. The wormlike micelle solutions were tested at concentrations of 150/75 and 50/25 mM CPyCl/NaSal. During mixing, a moderately elevated temperature was applied to reduce viscosity and aid in uniform mixing. After the solutions were fully dissolved, approximately 20–30 min, they were allowed to settle at room temperature for at least 24 h before any experiments were performed to allow air bubbles introduced during mixing to rise out of the fluid. The detailed shear rheology of these fluids can be found elsewhere (Bhardwaj et al. 2007a); however, for completeness, the zero shear viscosity, relaxation time and storage modulus for each of the fluids are listed in Table 1. The surface tension for the CPyCl/NaSal micelle solutions tested was taken to be its equilibrium value for solutions above the CMC, $\sigma = 0.032$ N/m (Akers and Belmonte 2006, Cooper-White et al. 2002). However, in any free surface flow containing surfactants, one must also consider the impact of dynamic surface tension on the experiment. As the fluid filament is stretched and a new surface is generated, surfactant molecules must diffuse from the bulk to populate the new surface. The result is a surface tension that is a function of the age of a given surface. However, because the timescales of the CaBER experiments described here are slow compared to the timescale of the dynamic surface tension (seconds vs. milliseconds;

Cooper-White et al. 2002) the use of the equilibrium value of the surface tension is a reasonable assumption and was therefore used in Eq. 2 in all of our subsequent calculations of the extensional viscosity.

The immiscible polymer blends were created by mixing low molecular weight Newtonian polyisobutylene (PIB) and polydimethylsiloxane (PDMS) oils with shear viscosities of $\eta = 14$ Pa s and $\eta = 12$ Pa s, respectively, at 25°C and at weight fractions of 90/10 and 80/20 PIB/PDMS. Disperse phase PDMS drops of uniform diameter were created in the bulk PIB phase using a shear rheometer (ARES RMS500) to shear the sample at a constant shear rate for strains of $\gamma = 5,000$ to ensure drop breakup. The size of the drops produced is determined by the critical capillary number

$$\text{Ca}_{\text{crit}} = \frac{\dot{\gamma} R \eta_b}{\sigma_{12}} \tag{4}$$

where R is the maximum radius of the drops that do not break, η_b is the viscosity of the bulk phase and σ_{12} is the interfacial tension between the dispersed and bulk phases. The critical capillary number has been shown to be a function of both the character of the flow (shear or extension) as well as the viscosity ratio, $\lambda = \eta_d/\eta_b$. For the present viscosity ratio of $\lambda = 0.9$, the critical capillary number has been found to be approximately $\text{Ca}_{\text{crit}} = 0.5$ in pure shear flows and $\text{Ca}_{\text{crit}} = 0.12$ in uniaxial extensional flows (Bentley and Leal 1986). A pendant drop experiment using a CAM200 (KVS Instruments Ltd.) was performed to measure the interfacial tension between the two fluids and found to be $\sigma_{12} = 2.2$ mN/m while the surface tension of the PIB bulk phase was found to be $\sigma = 26$ mN/m. For shear rates of $\dot{\gamma} = 11$ s^{-1} nominal drop sizes of $D = 14$ μm were produced. It should be noted that the droplet size is below the resolution limit of the laser micrometer used in the CaBER measurements; therefore, the effect of individual droplets during the final stages of filament breakup could not be observed.

The linear viscoelastic response of both the pure PDMS and PIB oils as well as the 80/20 PIB/PDMS and 90/10 PIB/PDMS are shown in Fig. 2. While the two single components show the expected monotonic increase of G' and G'' with frequency for melts close to their terminal relaxation regime, the blends show a typical shoulder in G' at low frequencies that is

Table 1 Parameters characterizing the rheology of the test fluids at $T_{\text{ref}} = 25°C$

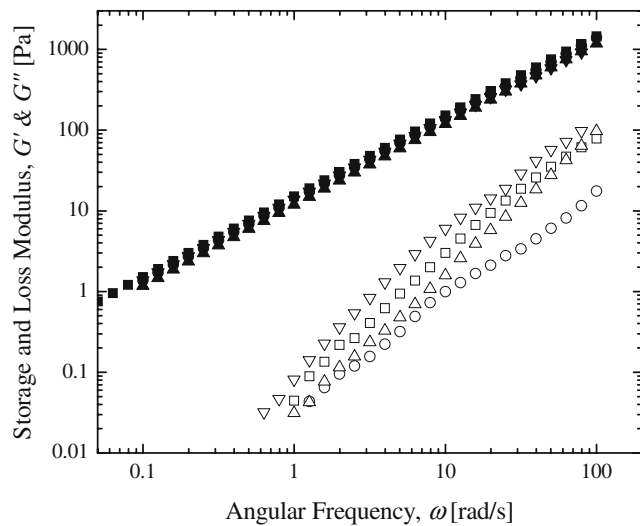| Fluid	Zero-shear viscosity η_0 [Pa-s]	Plateau modulus G [Pa]	Relaxation time λ [s]	Surface tension σ [mN/m]
150/75 mM CPyCl/NaSal	30	60	0.50	32
50/25 mM CPyCl/NaSal	1.0	4.2	0.27	32
1 wt.% PAA in water	2.9	14.5	0.2	72

Fig. 2 Linear viscoelasticity measurements of ▼ the 80%/20% PIB/PDMS solution, ■ the 90%/10% PIB/PDMS solution, the pure ● PIB and ▲ PDMS fluids. The hollow symbols represent the storage modulus G' while the filled symbols represent the loss modulus G''

related to the additional relaxation process of the shear-induced deformation of the droplet's elastic interface (Palierne 1990; Van Puyvelde and Moldenaers 2006). The elasticity of the droplet's interface has also been shown to result in strain hardening of the fluids extensional viscosity in the startup of uniaxial elongational flows (Oosterlinck et al. 2005).

Results and discussion

Polymer solutions

For the case of a homogeneous polymer solution, the results from CaBER experiments are insensitive to step-stretch parameters and the resulting extensional preconditioning before the onset of capillarity driven thinning. As demonstrated in the numerical simulations of Clasen et al. (2006) and Entov and Hinch (1997), these solution systems quickly approach the ideal elasto-capillary balance, independent of the initial state of stress induced by the step-stretch. The elasto-capillary thinning is dominated by the extensional relaxation time, λ_E, and consequently, a constant extension rate of $\dot{\varepsilon} = 2/3\lambda_E$ is achieved and very similar transient apparent extensional viscosities, $\eta_E(t)$, are calculated from the diameter decay. This can clearly be seen in the experimental results for the 1 wt.% PAA

solution in Figs. 3 and 4. These CaBER experiments were conducted with end plates of $D_0 = 3$ mm and the initial aspect ratio was fixed at $L_0/R_0 = 1$. The pre-stretch conditions were varied to cover a range of Weissenberg numbers as well as final aspect ratios. It is evident from Fig. 3 that all diameter curves approach the exponential thinning term of Eq. 3; moreover, they all thin with the same exponential coefficient $1/(3t\lambda_E)$ independent of pre-stretch conditions. This becomes even more apparent in Fig. 4 where the apparent viscosities calculated from the diameter data of Fig. 3 are plotted as a function of the Hencky strain $\varepsilon = 2\ln(D_0/D)$. From these experiments and previous numerical simulations, we can conclude that the viscosity evolution of polymer solutions is principally independent of the pre-stretch history once the elasto-capillary balance has been reached.

Unfortunately, the majority of early publications on capillary breakup experiments dealt with polymer solutions and helped to reinforce a misconception that all complex fluids are independent of the pre-stretch conditions in a CaBER experiment. However, polymeric solutions present only a small fraction of possible fluids to be tested with the CaBER (although probably the easiest systems to deal with theoretically). In the following sections, we present two classes of fluids for which this apparent pre-stretch independence of the CaBER experiment is not fulfilled.
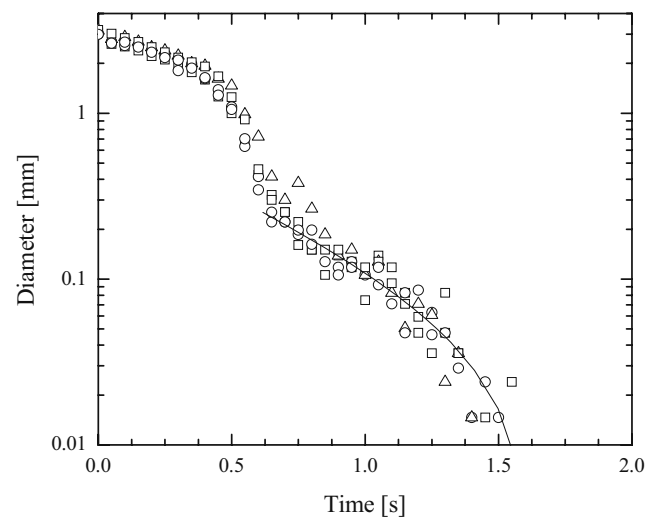

Fig. 3 Measurements of diameter as a function of time for a series of CaBER experiments with a 1% aqueous PAA solution. The data include step-stretch experiments with a fixed Weissenberg number of Wi = 0.5 and final stretch ratios of □ $L/R_0 = 3$, ○ $L/R_0 = 5$, △ $L/R_0 = 7$, ▽ $L/R_0 = 10$, and ◇ $L/R_0 = 15$ as well as a fit of the $L/R_0 = 5$ data with the functional form proposed in Eq. 3
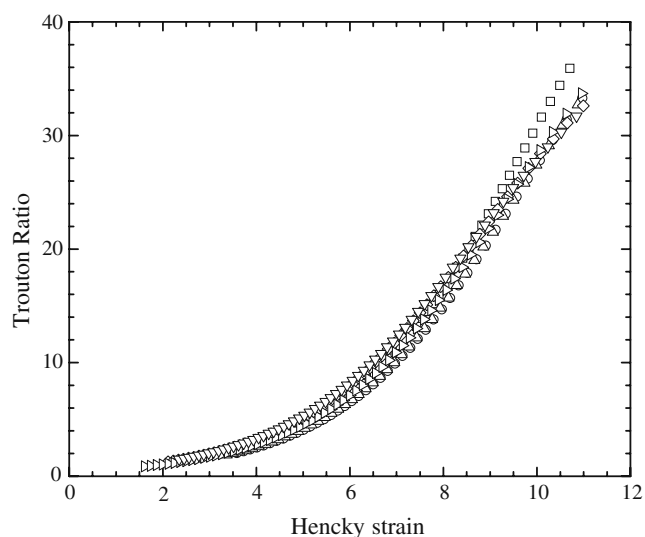
Fig. 4 Measurements of Trouton ratio as a function of Hencky strain for a series of CaBER experiments with a final stretch ratio of $L/R_0 = 10$ for 1 wt.% PAA solution and step-stretch Weissenberg numbers of: $\triangleright$ $Wi = 0.5$, $\square$ $Wi = 1$, $\circ$ $Wi = 3$, and $\triangle$ $Wi = 5$ as well as data for fixed $Wi = 0.5$ and final stretch ratios of $\lozenge$ $L/R_0 = 3$, $\triangledown$ $L/R_0 = 5$ and $\triangleright$ $L/R_0 = 10$

Wormlike micelle solutions

In Fig. 5a, a representative set of CaBER experiments for the 150/75 mM CPyCl/NaSal wormlike micelle solutions are presented for a series of Weissenberg numbers stretched to a constant final stretch length ratio of $L_f/R_0 = 10$, while in Fig. 5b, the Weissenberg number of the step-stretch is held fixed at Wi = 5 and the fluids are stretched to a range of final lengths L_f. In all cases, the radius of the plates was $R_0 = 1.5$ mm and the initial aspect ratio was fixed at $L_0/R_0 = 1$. The raw diameter data was fitted using the functional form in Eq. 3, and the results are superimposed over the data in Fig. 5. It should be noted that the initial step-stretch, starting at $t = 0$, is included in the experimental data, but not for the fit. The step-stretch can be clearly delineated from the capillary drainage regime by the change in slope of the diameter decay. The fit was then differentiated in order to calculate the apparent extensional viscosity as described by Eqs. 2 and 3. At intermediate times in the diameter decay, the extensional relaxation time was calculated from the fit parameters as described above.

The effect of increasing the Weissenberg number of the step-stretch can be clearly seen in Fig. 5a. As the step-stretch Weissenberg number was increased from Wi = 0.5 to Wi = 3, the diameter was observed to decay much more quickly with time; however, further increases in the step-stretch Weissenberg number

above Wi > 3 do not appear to have a significant impact on the CaBER experiments. In Fig. 5b, the step-stretch Weissenberg number was held fixed at Wi = 5, but the final stretch length was varied; these experiments are within the range where the extensional viscosity is insensitive to changes in Weissenberg number. The rate of diameter decay was found to increase with increasing final step-stretch length. It should be noted that in the case of low aspect ratio stretches, it can take some time after
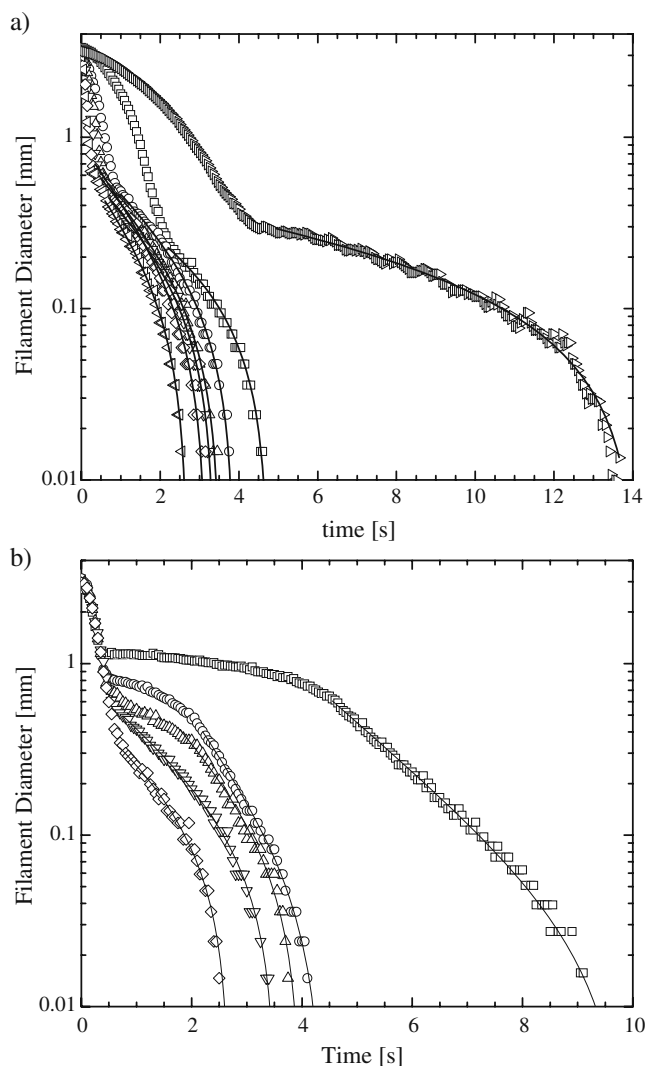
a)

b)

Fig. 5 Measurements of diameter as a function of time for a series of CaBER experiments with a wormlike micelle solution of 150 mM CPyCl, 75 mM NaSal and 100 mM NaCl in water. Included in **a** are step-stretch with a final stretch ratio of $L/R_0 = 10$ and Weissenberg numbers of $\triangleright$ $Wi = \lambda\dot{\varepsilon} = 0.5$, $\square$ Wi = 1, $\circ$ Wi = 3, $\triangle$ Wi = 5, $\triangledown$ Wi = 7, $\lozenge$ Wi = 10, and $\triangleleft$ Wi = 12. Included in **b** are step-stretch with a fixed Weissenberg number of Wi = 5 and final stretch ratios of $\square$ $L/R_0 = 3$, $\circ$ $L/R_0 = 5$, $\triangle$ $L/R_0 = 7$, $\triangledown$ $L/R_0 = 10$, and $\lozenge$ $L/R_0 = 15$

the cessation of the step-stretch for a fluid filament to form and capillary drainage to begin. This can be observed as a knee in the diameter data at early times in Fig. 5b for final stretch lengths less than $L_f/R_0 \leq 7$.

In Fig. 6, the apparent Trouton ratio which is the *apparent* extensional viscosity over shear viscosity, $Tr = \eta_E/\eta$, is plotted as a function of Hencky strain, $\varepsilon = 2\ln(D_0/D)$. The Trouton ratios were c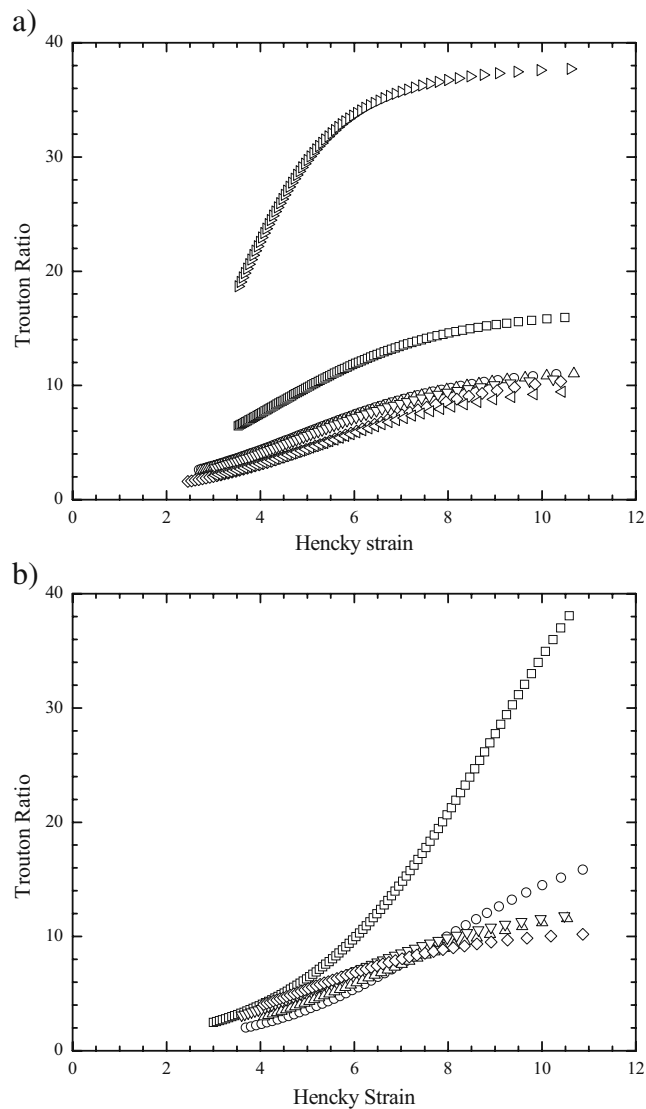alculated from the data sets presented in Fig. 5 and, there-fore, show very similar trends. In Fig. 6a, the worm-like micelles solutions were stretched to a constant final length of $L_f/R_0 = 10$ as the Weissenberg number was varied. Up to a Weissenberg num-ber of Wi = 3, the Trouton ratio was observed to decrease sharply before becoming insensitive to further increases to the step-stretch Weissenberg number above Wi > 3. The results show that the exten-sional viscosity measurements for these wormlike mi-celle solutions can differ by a factor of four depending on the Weissenberg number that one chooses for the initial step-stretch profile. In Fig. 6b, the Weissenberg number was held constant at Wi = 5 and the final length, L_f, was increased. The steady-state Trouton ratio was found to decrease by more than a factor of four as the stretch length was increased from $L_f/R_0 = 3$ to $L_f/R_0 = 7$. For stretches greater than $L_f/R_0 > 7$ little variation was observed in the extensional viscosity. Step-stretches much beyond $L_f/R_0 > 15$ were not successful as they would often fail through a rupture of the filament before the cessation of the step-strain.

The same procedure outlined above was used to determine the extensional viscosity of the 50/25 mM CPyCl/NaSal solutions from the measurements of their diameter decay with time. Similar extensional viscosity trends with increasing step-stretch rate and length were observed for both of the wormlike micelle solutions tested. As seen in Fig. 7, for a fixed Weissenberg num-ber of Wi = 3, as the stretch length was increased from $L_f/R_0 = 3$ to $L_f/R_0 = 7$, the extensional viscosity was reduced by a factor of about two. Beyond a stretch length of $L_f/R_0 > 7$, no further changes in the exten-sional viscosity were observed. Although not shown here for the purpose of brevity, the extensional viscos-ity of the 50/25 mM CPyCl/NaSal solutions showed a similar decay with increasing Weissenberg number and a fixed stretch length.

The existence of critical Weissenberg numbers and stretch ratios for wormlike micellar solutions during pre-stretch can also be seen in the extensional relax-ation times λ_E that were obtained from the fits of Eq. 3 to the experimental data in Fig. 5. In Fig. 8, these relaxation times, normalized by the constant shear re-laxation time λ, for both the 150/75 and the 50/25 mM CPyCl/NaSal are presented as a function of the step-stretch Weissenberg number. Similar to the extensional viscosity measurements, the extensional relaxation times of the wormlike micelle solutions were insensitive to the step-stretch Weissenberg number above Wi > 3 but were found to show a nearly exponentially decay with increasing Weissenberg below the critical value of Wi = 3. In terms of final stretch length, the data in
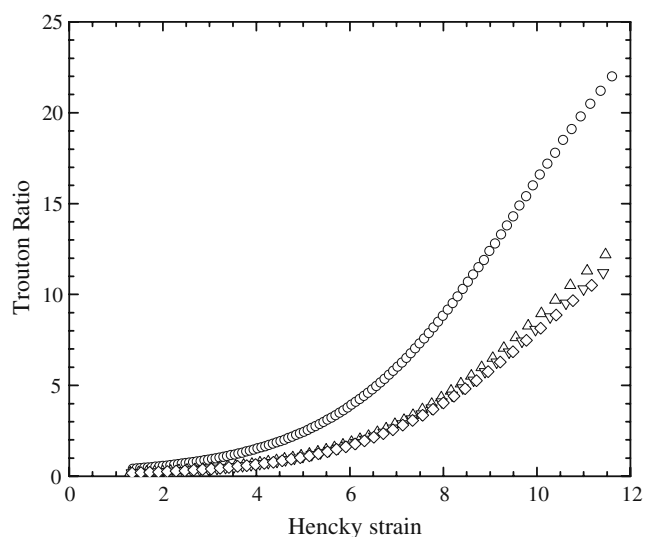

Fig. 6 Measurements of Trouton ratio as a function of Hencky strain for 150/75 mM CPyCl/NaSal wormlike micelle solution for a series of CaBER experiments. The data include (**a**) stretches with a constant final stretch ratio of $L/R_0 = 10$ and varying step-stretch Weissenberg numbers of ▷ Wi = 0.5, □ Wi = 1, ○ Wi = 3, △ Wi = 5, ▽ Wi = 7, ◇ Wi = 10, and ◁ Wi = 12 and **b** stretches with a constant step-stretch Weissenberg number of Wi = 5 and varying final stretch ratios of: □ $L/R_0 = 3$, ○ $L/R_0 = 5$, △ $L/R_0 = 7$, ▽ $L/R_0 = 10$, and ◇ $L/R_0 = 15$

Fig. 7 Measurements of Trouton ratio as a function of Hencky strain for a series of CaBER experiments of the 50/25 mM CPyCl/NaSal wormlike micelle solution with a fixed step-stretch Weissenberg numbers of Wi = 3.0 and a final stretch ratio of ○ $L/R_0 = 3$, △ $L/R_0 = 5$, ▽ $L/R_0 = 7$, and ◇ $L/R_0 = 10$

Fig. 9 suggest that the extensional relaxation time of wormlike micelle solutions can be even more strongly affected by changes in the final step-stretch length than changes to Weissenberg number. Again, above a critical value of $L_f/R_0 > 7$, the relaxation times were found to be insensitive to an increase of the final stretch length L_f/R_0 but show a strong decay of the relaxation time when increasing from $L_f/R_0 = 3$ to $L_f/R_0 = 7$,
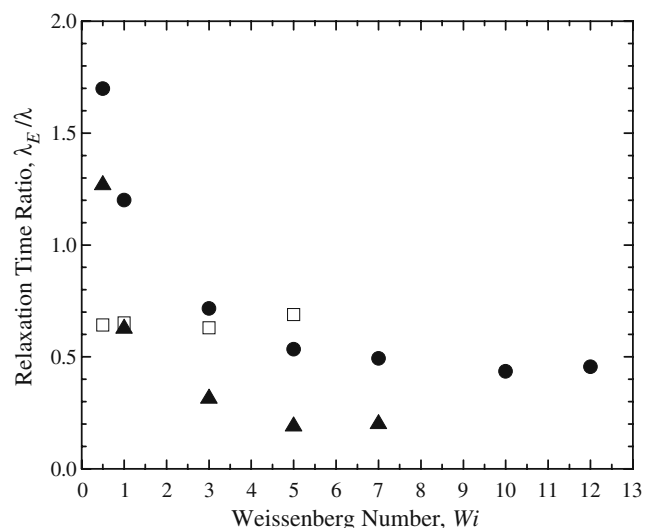
for both the 150/75 and the 50/25 mM CPyCl/NaSal solutions, respectively.

As a point of comparison, the extensional relaxation times obtained for the 1 wt.% PAA solution were superimposed over the data shown in Figs. 8 and 9. Unlike the wormlike micelle solutions, the extensional rheology of the PAA solution measured in CaBER was found to be insensitive to changes in either the Weissenberg number or the duration of the step-stretch. This observation is consistent with results found in our group for other polymer solutions and theory although a value slightly less then the theoretically predicted $\lambda_E/\lambda = 1$ was observed.

Again it is important to note that most of the CaBER experiments conducted to obtain a relaxation time that have been published to date have been for polymer solutions, which are insensitive to step-stretch conditions. One might, therefore, expect that the same should be true for wormlike micelle solutions or, as described in subsequent sections, immiscible polymer blends. However, our results present clear evidence that the step-stretch, which is required to obtain a viable fluid filament in CaBER, is likely to affect the size, aggregation number, or morphology of the wormlike micelle and can have a very strong effect on the response of wormlike micelle solutions in extensional flows. The observations suggest that higher Weissenberg numbers (Wi > 3) and larger strain step-stretches ($L_f/R_0 > 7$) in CaBER measurements produce the most reliable and repeatable measurements of extensional viscosity
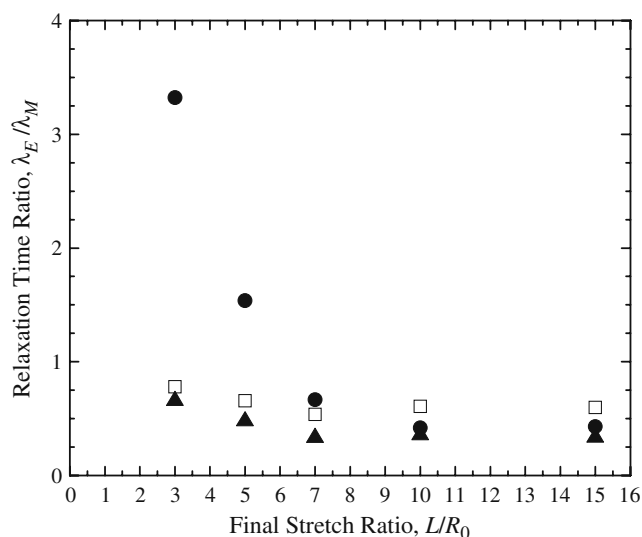

Fig. 8 Measurements of the relaxation time ratio λ_E/λ as a function of step-stretch Weissenberg number for a series of CaBER experiments. The data include: ● the 150 mM CPyCl solutions to a final stretch ratio of $L/R_0 = 10$, ▲ the 50 mM CPyCl solution with $L/R_0 = 7$, and □ the 1 wt.% PAA solution with $L/R_0 = 7$

Fig. 9 Measurements of the relaxation time ratio λ_E/λ as a function of final stretch ratio for a series of CaBER experiments. The data include: ● the 150 mM CPyCl solutions at a Weissenberg number of Wi = 5, ▲ the 50 mM CPyCl solution at Wi = 3, and □ the 1 wt.% PAA solution at Wi = 3

and relaxation time for wormlike micelle solutions. However, it is important to note that these observations may not be universal for all self-assembling systems. Furthermore, it is not clear in which morphological state the wormlike micellar system is in this regime of step-stretch experiments that gives results for the capillary thinning that are insensitive to the stretch history. In fact, it is the low Weissenberg number, small step-stretch measurements that agree more closely with the filament stretching measurements of these wormlike micelle solutions (Bhardwaj et al. 2007a). The sensitivity of the extensional rheology measurements of wormlike micelle solutions to the dynamics of the step-stretch parameters is a bit disconcerting because the variability of the measurements makes interpretation of the data and determination of the true extensional viscosity of these wormlike micelle solutions using CaBER very difficult. With fluids so sensitive to precise kinematics of stretch, these measurements suggest that filament stretching measurements would be more appropriate because the extension rate is held constant over the entire experiment. Unfortunately, filament stretching measurements are limited to more viscous solutions and often result in filament failure before a steady-state extensional viscosity can be measured. It is, thus, an open question as to what the best procedures should be to investigate the extensional properties for self-assembling systems. What is clear, however, is that a sensitivity analysis to the step-stretch parameters must be performed for CaBER measurements of all self-assembling systems.

Immiscible polymer blends

In this section, we will investigate the effect of pre-conditioning on the extensional viscosity measurements for a series of immiscible polymer blends. As seen in Fig. 2, the low molecular weight oils used in these polymer blends are essentially Newtonian. However, Oosterlinck et al. (2005) showed with filament stretching extensional rheology experiments that for immiscible polymer blends the elasticity of the fluid–fluid interface can result in a strain-hardening of the extensional viscosity in transient homogeneous uniaxial elongational flows as the droplets are deformed by the flow and an interfacial stress is accrued (Oosterlinck et al. 2005). Their experiments showed that the effect of the droplets can be quite significant. For a 15% disperse phase of polystyrene in polymethylmethacrylate, the interfacial stress was found to account for as much as 20% of the total stress developed within the fluid filament.

However, even though immiscible polymer blends have been found to produce an elastic response in extension which is quite similar to both the polymer solutions and the wormlike micellar systems discussed in the previous sections, they are expected to show a different behavior in CaBER experiments. The response to capillary thinning should be much closer to that of the Newtonian matrix fluid, PIB, than to an Oldroyd-B fluid, and the morphology is likely to be affected by the precise extensional flow profile. In particular, the latter point makes CaBER experiments of polymer blends extremely sensitive to the step-stretch parameters used to produce the initial filament. The filament stretching extensional rheology experiments of Oosterlinck et al. (2005), with a constant extension rate, represent, in principle, the step-stretch that is initially imposed in the CaBER experiments. However, after the step-stretch the dynamics change as the balance of interfacial tension and extensional stresses during the actual CaBER experiment dictate the evolution of the filament diameter with time once the filament has been formed.

Experimental results for immiscible polymer blends

In Fig. 10, the diameter is plotted as a function of time for a series of CaBER experiments performed on both the 80/20 and the 90/10 PIB/PDMS blends as well as the PIB oil which serves as the matrix fluid for both samples. In all of these experiments the plate radius was fixed at $R_0 = 2$ mm. It should be noted that the results in Fig. 10 are representational experiments chosen from a set of between five and ten independent experiments at each experimental condition. As expected, the diameter of the Newtonian PIB oil as shown in Fig. 10b was observed to decay linearly with time resulting in a nearly constant viscosity that is independent of the step-stretch parameters.

In Fig. 10a, the effect of either varying the initial step-stretch rate is demonstrated. The initial and the final length of the 80/20 PIB/PDMS filament was fixed at $L_0/R_0 = 1.0$ and $L_f/R_0 = 5.0$, respectively, and the extension rate of the step-stretch was varied between $1\,\mathrm{s}^{-1} < \dot{\varepsilon} < 20\,\mathrm{s}^{-1}$. The stretch rates in Fig. 10a were chosen such that they would span the critical capillary number of the drop. As seen in Fig. 10a, at the lowest initial extension rate of $\dot{\varepsilon} = 1\,\mathrm{s}^{-1}$ which is below the extension rate at the critical capillary number for drop breakup, $\dot{\varepsilon}_{\mathrm{crit}} = 2.05\,\mathrm{s}^{-1}$, the decay of the fluid filament starts off with a constant slope, similar to a purely Newtonian behavior, but slows a little at longer times resulting in a modest strain hardening beginning at a strain of approximately $\varepsilon \approx 3$. As the extension
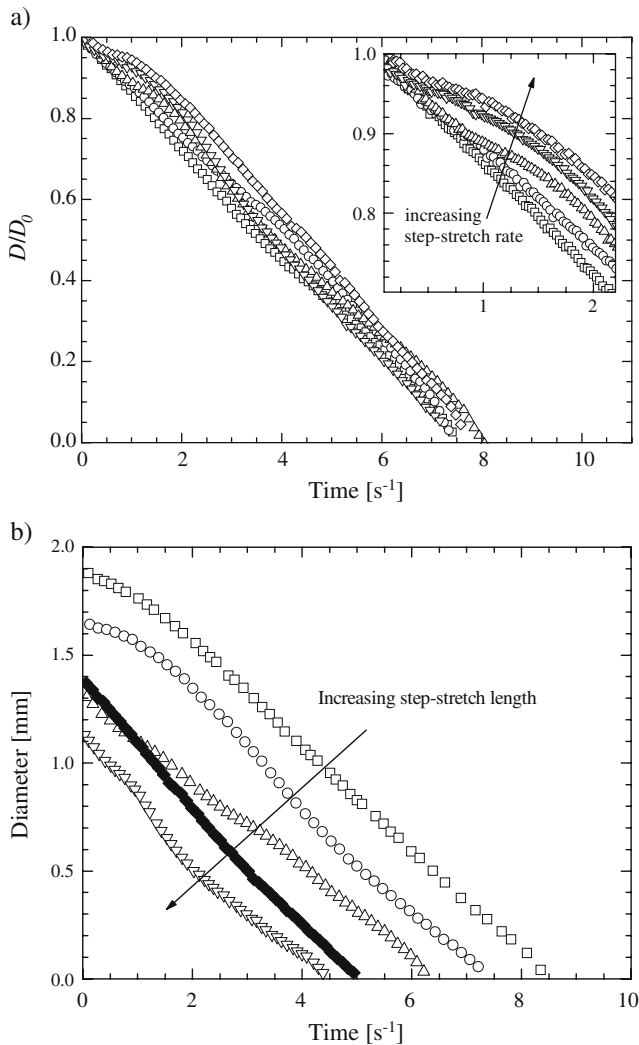
a)

b)

Fig. 10 Measurements of diameter as a function of time for a series of CaBER experiments with an immiscible polymer blend of **a** 80%/20% PIB/PDMS and **b** 90%/10% PIB/PDMS having a viscosity ratio of $\lambda = 0.9$. Included in **a** are step-stretches with a constant final stretch ratio of $L_f/R_0 = 5$ and imposed extension rates of ■ $\dot{\varepsilon} = 1\,\mathrm{s}^{-1}$, ● $\dot{\varepsilon} = 2\,\mathrm{s}^{-1}$, ▲ $\dot{\varepsilon} = 5\,\mathrm{s}^{-1}$, ▼ $\dot{\varepsilon} = 10\,\mathrm{s}^{-1}$, and ♦ $\dot{\varepsilon} = 20\,\mathrm{s}^{-1}$. Included in **b** are step-stretches with a fixed extension rate of $\dot{\varepsilon} = 24\,\mathrm{s}^{-1}$ and final stretch ratios of ■ $L_f/R_0 = 4$, ● $L_f/R_0 = 5$, ▲ $L_f/R_0 = 6.25$, and ▼ $L_f/R_0 = 7.5$. The closed symbols represent for comparison the thinning of the pure PIB matrix after a step-stretch extension rate with $\dot{\varepsilon} = 24\,\mathrm{s}^{-1}$ to a final ratio of $L_f/R_0 = 6.25$

rate of the step-stretch is increased beyond that of the critical capillary number, a knee develops in the data at early times after an initial decay following the cessation of the step-stretch as seen in the insert of Fig. 10a. Although direct observations of the drop deformation were not possible, the data suggest that for stretch rates resulting in a capillary number larger than the critical capillary number, the initial step-stretch deforms the PDMS drops. Upon cessation of the imposed

extensional flow, the extension rate slows dramatically and the deformed droplets retract returning some of their stored elastic potential energy to the flow and dramatically slowing the viscocapillary thinning of the fluid filament resulting in the initial increase observed in the apparent extensional viscosity. As described previously, a Matlab routine was used to fit the diameter data with a spline in order to minimize the impact of the noise in the data while still capturing all the interesting features of the diameter decay. The resulting fit was then differentiated and inserted into Eq. 2 in order to calculate the transient extensional viscosity. As seen in Fig. 11a, the knee in the diameter data results in a dramatic increase in the extensional viscosity at early times and small strains. The enlarged insert of Fig. 11a shows that the size of this knee and the resulting extensional viscosity overshoot is observed to increase with increasing extension rate during the initial step-stretch. This is in accordance with an increased deformation of the droplets after the stretch as their possibility to relax during the step-stretch decreases with increasing rate. In addition to the knee at early times, the diameter data for the large extension rate cases exhibits a number of less pronounced diameter decay rate fluctuations which result in a number of additional peaks in the extensional viscosity as the filament decays.

Similar results are also observed for an increasing initial step deformation in Figs. 10b and 11b. Here, the extension rate of the step-stretch was fixed at $\dot{\varepsilon} = 24\,\mathrm{s}^{-1}$, and the filament was stretched from an initial aspect ratio of $L_0/R_0 = 1.0$ to a final filament length that was varied between $4 \le L_f/R_0 \le 7.5$. The concentration of PIB and PDMS were varied from Fig. 10a, b to 90/10 PIB/PDMS to demonstrate that the sensitivity of these immiscible polymer blends to step-stretch conditions is robust over a range of drop concentrations. Both the size of the knee in the diameter data and the overshoot in the extensional viscosity were found to initially increase with increasing step-stretch lengths up to $L_f/R_0 = 5$. However, beyond a critical step-stretch length of $L_f/R_0 > 5$, the overshoot in extensional viscosity was found to decrease again with increasing stretch length.

The decrease of the overshoot in extensional viscosity at higher initial step deformation can be associated with a breakup of droplets during the initial step-stretch. In accordance with Stone and Leal (1989) who, for a viscosity ratio of $\lambda = 0.9$, give a critical deformation for the breakup of quasistatic droplets after an affine deformation of the order $\varepsilon_{crit} = O(3)$, we expect to observe an effect of droplet break up on our CaBER experiment when reaching this critical deformation limit. The extension rate during the initial
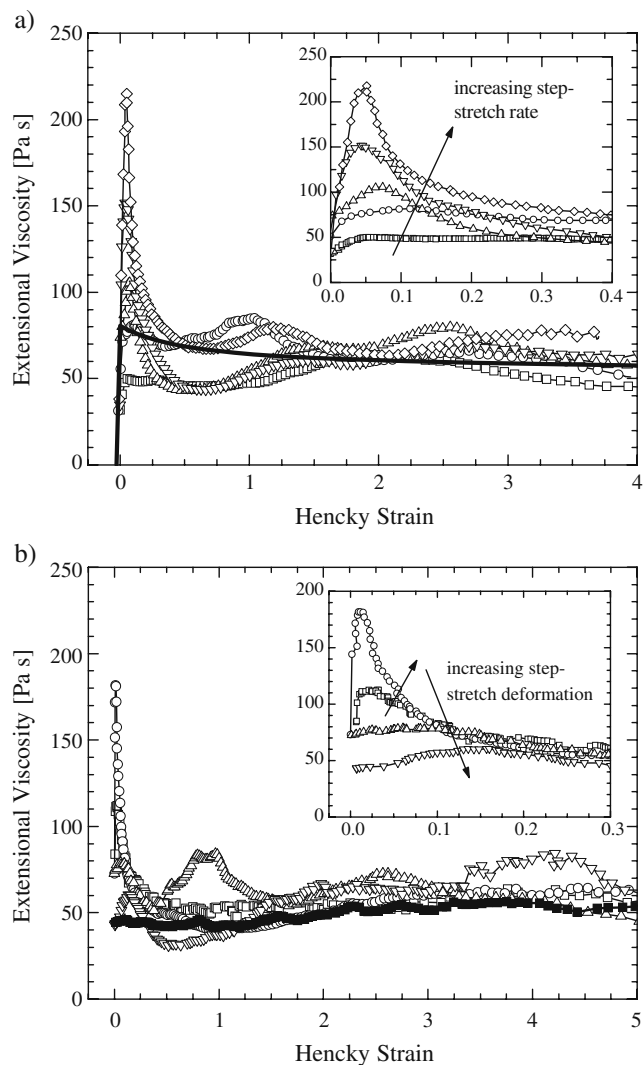
a)

b)

Fig. 11 Measurements of extensional viscosity as a function of accumulated Hencky strain for a series of CaBER experiments with an immiscible polymer blend of **a** 80%/20% PIB/PDMS and **b** 90%/10% PIB/PDMS with viscosity ratios of $\lambda = 0.9$. Included in **a** are step-stretch with a final stretch ratio of $L_f/R_0 = 5$ and imposed extension rates of ■ $\dot{\varepsilon} = 1\,\mathrm{s}^{-1}$, ● $\dot{\varepsilon} = 2\,\mathrm{s}^{-1}$, ▲ $\dot{\varepsilon} = 5\,\mathrm{s}^{-1}$, ▼ $\dot{\varepsilon} = 10\,\mathrm{s}^{-1}$, ◆ $\dot{\varepsilon} = 20\,\mathrm{s}^{-1}$ and the predictions based on a Maffettone and Minale model for $\dot{\varepsilon} = 10\,\mathrm{s}^{-1}$. Included in **b** are step-stretch with a fixed extension rate of $\dot{\varepsilon} = 24\,\mathrm{s}^{-1}$ and final stretch ratios of ■ $L_f/R_0 = 4$, ● $L_f/R_0 = 5$, ▲ $L_f/R_0 = 6.25$, and ▼ $L_f/R_0 = 7.5$ as well as the pure PIB to ◆ $L_f/R_0 = 5$ and the predictions based on a Maffettone and Minale model for $\dot{\varepsilon} = 24\,\mathrm{s}^{-1}$

step-stretch in Figs. 10b and 11b was $\dot{\varepsilon} = 24\,\mathrm{s}^{-1}$, well beyond the extension rate at the critical capillary number for drop breakup, which calculates for our drop diameters to $\dot{\varepsilon}_{\mathrm{crit}} = 2.64\,\mathrm{s}^{-1}$. For rates above the critical capillary number the droplets are expected to deform affinely with the matrix flow (Bentley and Leal 1986; Stone and Leal 1989); and we can, therefore, directly estimate from the diameters after the step-stretch in

Fig. 10b the deformation of the droplets. With a deformation of $\varepsilon \sim 3.1$ obtained in this way for the critical case of $L_f/R_0 = 6.25$ in Fig. 10b, for which a decrease in the viscosity overshoot is observed, we indeed meet the critical conditions given by Stone and Leal during the initial step-stretch and the viscosity overshoot is, therefore, smaller as less elastic energy is stored in the deformed droplet surface.

Figures 10a and 11a support the prediction not only that rate is not the sole condition for breakup during the step-stretch but also that a critical deformation needs to be exceeded. Although all higher initial step-stretch rates in Figs. 10a and 11a are beyond the critical rate for drop breakup, the deformation fixed at $L_f/R_0 = 5$ (leading to a value of $\varepsilon \sim 2.3$ for affine deformed drops) is not high enough to break the drops, resulting in an ever increasing viscosity overshoot with rate.

Modeling for immiscible polymer blends

The formation of the knee in the diameter decay data and the resulting extensional viscosity peaks observed at small strains demonstrates that, like the wormlike micelle solutions described in the previous section, the choice of step-stretch parameters used to form the fluid filament in CaBER measurements of immiscible polymer blends can have a significant impact on the resulting extensional viscosity measurements. In order to try to understand the CaBER results from first principles and to quantify the effects of the above proposed effects of deforming droplets on the thinning dynamics of a CaBER experiment during the initial step-stretch and the following capillary thinning, we used the Maffettone and Minale model (1998).

The Maffettone and Minale model (1998) was originally developed in order to determine droplet deformation resulting from an arbitrary flow around a droplet. The model makes two basic assumptions. First, that the droplet remains ellipsoidal at all time and second, that the drop does not break up. It is, thus, only truly applicable in flows below the critical capillary number. The Maffettone and Minale model tracks the evolution of the drop shape tensor S through the following equation

$$\frac{dS}{dt} - \boldsymbol{\Omega} \cdot S + S \cdot \boldsymbol{\Omega} = -\frac{f_1}{\tau}\left[S - g\left(S\right)I\right] + f_2\left(E \cdot S + S \cdot E\right). \quad (5)$$

The Eigenvalues of S, $\lambda_{s,1}$ and $\lambda_{s,2}$, represent the square of the principal axis of the ellipsoid. Both f_1 and f_2 are

empirical constants which are functions of the viscosity ratio, λ, and the capillary number, Ca, of the flow

$$f_1 = \frac{40\,(\lambda+1)}{(2\,\lambda+3)\,(19\,\lambda+16)},$$
$$f_2 = \frac{5}{(2\lambda+3)} + \frac{3\,Ca^2}{2+6\,Ca^2}, \qquad (6)$$

while E is the shear rate tensor and Ω is the vorticity tensor. To ensure conservation of drop volume, the variable g is defined as $g\,(S) = 3III_s/II_s$ where II_s and III_s are the second and third invariants of the drop shape tensor S, respectively.

The step-stretch is an imposed flow with a constant extension rate. Matlab was used to solve Eq. 5 for the shear rate and strain imposed during the step-stretch and the resulting drop shape was in turn used to set the initial conditions needed to simulate the droplet deformation under a typical CaBER experiment. To solve for the resulting diameter decay during the CaBER experiment the extensional stresses, both viscous and elastic, were balanced with the surface stresses generated by the decaying fluid filament, resulting in

$$3\eta_b \dot{\varepsilon} + \tau_{\text{drop}} = \frac{2\sigma}{D_{\text{mid}}}. \qquad (7)$$

Substituting in for the extension rate from Eq. 1 we find an evolution equation for the diameter of the fluid filament

$$\frac{dD_{\text{mid}}}{dt} = -\frac{\sigma}{3\eta_b} + \frac{D_{\text{mid}}\,\tau_{\text{drop}}}{6\eta_b}. \qquad (8)$$

The elastic stress due to the deformation of the surface of the droplets undergoing an uniaxial elongation is given by (Wetzel and Tucker 1999)

$$\tau_{\text{drop}} = \frac{\phi\,\sigma_{12}}{L_c} \left(\frac{1 - \left(\frac{\lambda_{s,1}}{\lambda_{s,2}}\right)^{\frac{1}{2a}}}{1 + 2\left(\frac{\lambda_{s,1}}{\lambda_{s,2}}\right)^{\frac{1}{2a}}} \right), \qquad (9)$$

where σ_{12} is the interfacial tension between the immiscible oils, ϕ is the volume fraction of drops and $L_c = V_d/S_d$ is the ratio of the volume to surface area of the droplet and represents a characteristic lengthscale of the droplets, $\lambda_{s,i}^{1/2}$ are the respective roots of the Eigenvalues of the drop shape tensor S that represent the lengths of the principal axis of the ellipsoidally deformed drop, while a is the necessary conversion factor to infer area information (necessary for the stress determination) from the shape components. Following Wetzel and Tucker (1999), a value of $a = 0.5977$ rep-

resents an exact solution for the case of a uniaxially deforming ellipsoid. The resulting coupled O.D.E.s for the filament diameter in Eq. 8 and the drop deformation in Eq. 5 were solved using Matlab for a number of different step-stretch conditions and are superimposed over the data in Fig. 11a.

The results of the numerical predictions give the overshoot in the extensional viscosity after the step-stretch that is directly related to the degree of droplet deformation. The step-stretch deformation rates imposed on the fluid filament are significantly larger than the initial extension rate experienced during the capillary drainage of the fluid filament. As a result, during the initial stages of CaBER right after the step-stretch, the simulations predict that the drops will slowly relax back towards spherical, returning elastic potential energy in the process. This accounts for the overshoot in the extensional viscosity and the decay with increased time and strain.

However, it should be noted that the simulations give only a qualitative prediction of the large initial overshoot in the experimentally observed extensional viscosity data seen in Fig. 11a. The initial overshoot, while related to the deformation of droplets within fluid filament, is most likely the result of a complex rearrangement of the fluid filament shape from an initial hourglass shape to a constant diameter slender fluid filament during the early times of the CaBER test. The gravitational effects that play an important role at these large initial diameters (and, therefore, Bond numbers far above unity; McKinley and Tripathi 2000) are not taken into account and, therefore, prevent a quantitative agreement of the simulation with experiments.

Another deviation of the simulation predictions from the capillary thinning experiments can be observed at smaller diameters and later times, where gravitational effects can safely be neglected. According to the simulations, at long times and large strains, the extension rate of the fluid filament and the capillary number on the droplets grows large and they begin to deform again. However, at this point, our calculations predict that the additionally stress accumulated within the droplet is small compared to the capillary stresses within the fluid filament and the model does not predict the slow down or viscosity overshoot observed once the critical capillary number of the droplets is reached. This is because the simple Minale model on which our calculations are based is strictly only valid for small droplet deformations and furthermore does not account for drop breakup at large capillary numbers.

The experimental results, however, show that at later times, the droplet deformation also has a strong impact

on the thinning dynamics of the filament. To illustrate this, it is helpful to plot the extensional viscosity not against the total accumulated strain as it is in Fig. 11 but against the strain rate as shown in Fig. 12. It can clearly be seen that at critical rates during the thinning dynamics the extensional viscosity rises significantly at a constant extensional rate level. This behavior (that relates to the secondary peaks in the data in Fig. 11) is directly described by Eq. 1, the elastocapillary balance that occurs during the stretching of an elastic component of our system. The closeness of the relaxation or extension rate, at which these phenomena are observed in Fig. 12, to that of the critical capillary number of droplet breakup in extension (that is also indicated in the figure) indicates that it is indeed the extension against the elastic tension of the deforming droplet surfaces and breakup of a fraction of droplets that causes the secondary peaks in viscosity and the variation in the diameter decay.

These measurements demonstrate just how sensitive CaBER measurements of immiscible polymer blends can be to the precise kinematics of the imposed step-stretch. Great care is clearly needed when analyzing and interpreting CaBER measurements of immiscible polymer blends because the results are complex and atypical of viscoelastic polymer or wormlike micelle solutions.
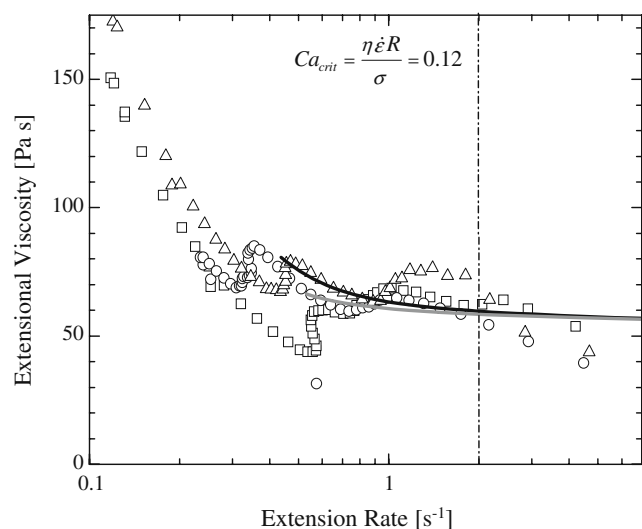

Fig. 12 Measurements of extensional viscosity as a function of strain rate for a series of CaBER experiments with an immiscible polymer blend of 80%/20% PIB/PDMS with viscosity ratios of $\lambda = 0.9$. The data include step-stretches with a final stretch ratio of $L_f/R_0 = 5$ and imposed extension rates of ■ $\dot{\varepsilon} = 2\,\mathrm{s}^{-1}$, ● $\dot{\varepsilon} = 10\,\mathrm{s}^{-1}$, ▲ $\dot{\varepsilon} = 20\,\mathrm{s}^{-1}$ and *solid lines* representing the predictions based on a Maffettone and Minale model (1998) for $\dot{\varepsilon} = 2\,\mathrm{s}^{-1}$ in *gray* and $\dot{\varepsilon} = 20\,\mathrm{s}^{-1}$ in *black*

Conclusions

Extensional rheometry measurement techniques for mid to low-viscosity viscoelastic fluids have only recently been developed into a commercially available tool with the introduction of the capillary breakup extensional rheometer. CaBER is an evolving technique which has been seeing increasing use in both industrial and academic settings. However, although a number of best practices have been suggested, a detailed study of the effect of step-stretch parameters on the measured extensional viscosity and relaxation time has not been performed. In this paper, the results from a series of experiments in which the final stretch length and the extension rate imposed for the step-stretch used to produce a viable filament for CaBER measurement were varied and their effects on the measured extensional viscosity and extensional relaxation time were recorded. A number of well-characterized viscoelastic fluids were chosen including two wormlike micelle solutions, a polymer solution and a number of immiscible polymer blends. The variety of these fluids allowed us to investigate the effect of step-stretch parameters on a number of different classes of viscoelastic fluids over a wide range of relaxation times and macromolecular morphologies.

Our experimental results demonstrate a strong dependence of extensional rheology on step-stretch conditions for both wormlike micelle solutions and immiscible polymer blends, however, the polymer solution tested was found to be insensitive to step-stretch parameters. Wormlike micelle solutions were particularly sensitive to both the strain rate and total strain imposed during the step-stretch. Both the extensional viscosity and the extensional relaxation time were found to decay quite strongly as the strain rate and the final stretch length were increased eventually reaching asymptotic values at high strain rates and final stretches. These observations were consistent for both of the surfactant concentrations examined although the sensitivity to the preconditioning was observed to differ slightly. These results present clear evidence that the step-stretch required to obtain a viable fluid filament in CaBER can affect the size, aggregation number or morphology of the wormlike micelle and have a very strong effect on the response of wormlike micelle solutions and other self-assembling systems in extensional flows. For the wormlike micelle solutions tested, a general criteria of Wi > 5 and $L_f/R_0 > 7$ was found for which step-stretch insensitive results could be achieved. It is important to note that these observations may not be universal for all self-assembling systems and a sensitivity analysis to

step-stretch parameters is strongly recommended for CaBER measurements of all self-assembling systems.

A number of immiscible polymer blends were studied using CaBER and the resulting extensional rheology was found to be quite complex. As the extension rate of the step-stretch was increased beyond the critical capillary number, a knee was observed to develop in the diameter decay data. The presences of the knee resulted in a dramatic increase in the extensional viscosity at early times and small strains. The initial and subsequent maxima in the extensional viscosity at larger strains were observed to increase with increasing extension rate of the step-stretch. To help analyze the data, a numerical simulation was performed using a Maffettone and Minale model (1998) to simulate the droplet deformation in a typical CaBER experiment. The model predictions confirmed our initial hypothesis that the extensional viscosity overshoot was due to the initial deformation of the droplets during the high capillary number step-stretch and the subsequent relaxation of the droplets back towards spherical during the early, low capillary number stages of CaBER. These measurements demonstrate just how sensitive CaBER measurements of immiscible polymer blends can be to the precise kinematics of the applied step-stretch.

The results presented in this paper clearly demonstrate for all three classes of fluids tested that great care is needed when analyzing and interpreting any CaBER measurement. Although it would be convenient to use CaBER as a point and click device for measuring extensional viscosity, one must recognize that the extension rate profile applied to the fluid filament is not constant with time, but can vary quite a bit over the course of a CaBER experiment. In the experiments presented in this paper, the speed and duration of the step-stretch required to form a fluid filament were found to impact the extensional viscosity measurements of both worm-like micelle solutions and immiscible polymer blends. Although a number of questions still remain as to what the best practices for CaBER measurements should be, it is clear that a sensitivity analysis to step-stretch parameters needs to be performed and analyzed if one hopes to use CaBER as anything other than a fluid indexer.

References

Agarwal US (2000) Effect of initial conformation, flow strength and hydrodynamic interaction on polymer molecules in extensional flows. J Chem Phys 113:3397–3403

Akers B, Belmonte A (2006) Impact dynamics of a solid sphere falling into a viscoelastic micellar fluids. J Non-Newton Fluid Mech 135:97–108

Anna SL (2000) Filament stretching of model elastic liquids. PhD thesis, Harvard University

Anna SL, McKinley GH (2001) Elasto-capillary thinning and breakup of model elastic liquids. J Rheol 45:115–138

Anna SL, McKinley GH (2008) Effect of a controlled pre-deformation history on extensional viscosity. Rheol Acta 47:841–859

Bazilevsky AV, Entov VM, Rozhkov AN (1990) Liquid filament microrheometer and some of its applications. In: Proc third European rheology conference. Edinburgh

Bentley BJ, Leal LG (1986) An experimental investigation of drop deformation and breakup in steady, two dimensional linear flows. J Fluid Mech 167:241–283

Bhardwaj A, Miller E, Rothstein JP (2007a) Filament stretching and capillary breakup extensional rheometry measurements of viscoelastic wormlike micelle solutions. J Rheol 51: 693–719

Bhardwaj A, Richter D, Chellamuthu M, Rothstein JP (2007b) The effect of preshear on the extensional rheology of wormlike micelle solutions. Rheol Acta 46:861–875

Clasen C, Plog JP, Kulicke WM, Owens M, Macosko C, Scriven LE, Verani M, McKinley GH (2006) How dilute are dilute solutions in extensional flows? J Rheol 50:849–881

Cooper-White JJ, Crooks RC, Boger DV (2002) A drop impact study of worm-like viscoelastic surfactant solutions. Colloids Surf A: Physicochem Eng Asp 210:105–123

Doyle PS, Shaqfeh ESG, McKinley GH, Spiegelberg SH (1998) Relaxation of dilute polymer solutions following extensional flow. J Non-Newton Fluid Mech 76:79–110

Edmond KV, Marquez M, Schofield AB, Rothstein JP, Dinsmore AD (2006) Stable jets of viscoelastic fluids and self-assembled cylindrical capsules by hydrodynamic focusing. Langmuir 22:9052–9056

Entov VM, Hinch EJ (1997) Effect of a spectrum of relaxation times on the capillary thinning of a filament of elastic liquid. J Non-Newton Fluid Mech 72:31–53

James DF, McLean BD, Saringer JH (1987) Presheared extensional flow of dilute polymer solutions. J Rheol 31:453–481

Kojic N, Bico J, Clasen C, McKinley GH (2006) Ex vivo rheology of spider silk. J Exp Biol 209:4355–4362

Larson RG (2000) The role of molecular folds and "preconditioning" in the unraveling of polymer molecules during extensional flow. J Non-Newton Fluid Mech 94:37–45

Larson RG (2005) The rheology of dilute solutions of flexible polymers: Progress and problems. J Rheol 49:1–70

Maffettone PL, Minale M (1998) Equation of change for ellipsoidal drops in viscous flows. J Non-Newton Fluid Mech 78:227–241

McKinley GH, Tripathi A (2000) How to extract the Newtonian viscosity from capilary breakup measurements in a filament rheometer. J Rheol 44:653–670

Oosterlinck F, Mours M, Laun HM, Moldenaers P (2005) Morphology development of a polystyrene/polymethylmethacrylate blend during start-up of uniaxial elongational flow. J Rheol 49:897–918

Palierne J-F (1990) Linear rheology of viscoelastic emulsions with interfacial tension. Rheol Acta 36:204–214

Papageorgiou DT (1995) On the breakup of viscous liquid threads. Phys Fluids 7:1529–1544

Plog JP, Kulicke WM, Clasen C (2005) Influence of the molar mass distribution on the elongational behaviour of polymer solutions in capillary breakup. Appl Rheol 15:28–37

Rodd LE, Scott TP, Cooper-White JJ, McKinley GH (2005) Capillary break-up rheometry of low-viscosity elastic fluids. Appl Rheol 15:12–27

Rothstein JP (2003) Transient extensional rheology of wormlike micelle solutions. J Rheol 47:1227–1247

Rothstein JP, McKinley GH (2002) Inhomogeneous transient uniaxial extensional rheometry. J Rheol 46:1419–1443

Smith DE, Chu S (1998) Response of flexible polymers to a sudden elongational flow. Science 281:1335–1340

Stelter M, Brenn G, Yarin AL, Singh RP, Durst F (2000) Validation and application of a novel elongational device for polymer solutions. J Rheol 44:595–616

Stone HA, Leal LG (1989) Relaxation and breakup of an initially extended drop in an otherwise quiescent fluid. J Fluid Mech 198:399–427

Van Puyvelde P, Moldenaers P (2006) Rheology and morphology development in immiscible polymer blends. In: Binding DM, Walters K (Eds) Rheology reviews. The British Society of Rheology, Aberystwyth

Vissmann K, Bewersdorff H-W (1990) The influence of pre-shearing on the elongational behavior of dilute polymer and surfactant solutions. J Non-Newton Fluid Mech 34:289–317

Wetzel ED, Tucker CL (1999) Area tensors for modeling microstructure during laminar liquid-liquid mixing. Int J Multiph Flow 25:35–61

Yesilata B, Clasen C, McKinley GH (2006) Nonlinear shear and extensional flow dynamics of wormlike surfactant solutions. J Non-Newton Fluid Mech 133:73–90